NASA CR-182,167

NASA Contractor Report 182167
AIAA-88-3076

NASA-CR-182167
19880016952

High Speed Inlet Calculations With Real Gas Effects

William J. Coirier
Sverdrup Technology, Inc.
NASA Lewis Research Center Group
Cleveland, Ohio

July 1988

Prepared for
Lewis Research Center
Under Grant NAS3-24105

NASA
National Aeronautics and
Space Administration

HIGH SPEED INLET CALCULATIONS WITH REAL GAS EFFECTS

William J. Coirier*

Sverdrup Technology, Inc.
NASA Lewis Research Center Group
Cleveland, Ohio 44135 U.S.A.

ABSTRACT

A two dimensional steady-state Navier-Stokes solver has been upgraded to include the effects of frozen and equilibrium air chemistry for applications to high speed flight vehicles. To provide a computationally economical first order approximation to the high temperature physics, variable thermodynamic data is used for the chemically frozen mode to allow for a variation with temperature of the air specific heats and enthalpy. For calculations involving air in chemical equilibrium, a specially modified version of the NASA Lewis Chemical Equilibrium Code, CEC, is used to compute the chemical composition and resultant thermo-chemical properties. The upgraded solver is demonstrated by comparing results from calorically perfect (C_p=constant), thermally perfect (frozen) and equilibrium air calculations for a variety of geometries, and flight Mach numbers.

INTRODUCTION

The two dimensional steady state Navier-Stokes solver that has been upgraded to account for first order real gas effects is the PARC2D code. The PARC2D code is a highly modified version of AIR2D[1] that has been made into a practical engineering analysis tool for propulsion oriented problems by Cooper, et. al.[2] of Sverdrup Technology at AEDC. PARC solves the Reynolds averaged Navier-Stokes equations using the approximate factorization algorithm of Beam and Warming[3]. To avoid the expense of inverting the large block banded matrix system of AIR2D, Pulliam[4] diagonalized the implicit operators, which resulted in signifigant improvements in computation time. Artificial dissipation was also added as proposed by Jameson[5] to improve convergence and shock capturing capability, which then resulted in the ARC2D series of codes. This code was then modified by Cooper et. al.[1] for use in solving propulsion oriented problems at the Arnold Engineering Development Center. These modifications resulted in the PARC series of codes.

The PARC codes are well validated and accepted and are in wide use by the aerodynamics community. Through the use of a unique method of grid patching and the segmented application of boundary conditions, the PARC series of codes are very useful for solving propulsion oriented problems. This solver was originally developed to calculate flows of a single constituent that is assumed to be a calorically perfect gas. This assumption is usually good for lower speed flows, but for high speed calculations with resultant high enthalpies, wall temperatures and heat transfer rates can be overpredicted. To permit more realistic calculations of high speed flows, this useful flow solver has been modified to account for flows of thermally perfect gases and flows where air is in thermal and chemical equilibrium.

ANALYSIS

PARC solves the Reynolds averaged Navier-Stokes equations on a curvilinear coordinate system written in divergence form, given below

$$\partial_t \vec{q} + \partial_x \vec{E} + \partial_y \vec{F} = Re^{-1}(\partial_x \vec{R} + \partial_y \vec{S}) \qquad (1)$$

where $\vec{q}$ is a vector containing the conservation variables:

$$\vec{q} = \begin{pmatrix} \rho \\ \rho u \\ \rho v \\ E \end{pmatrix} = \begin{pmatrix} q_1 \\ q_2 \\ q_3 \\ q_4 \end{pmatrix} \qquad (2)$$

The vectors $\vec{E}$ and $\vec{F}$ are the inviscid flux vectors:

$$\vec{E} = \begin{pmatrix} \rho u \\ \rho u^2 + p \\ \rho u v \\ u(E+p) \end{pmatrix} \qquad \vec{F} = \begin{pmatrix} \rho v \\ \rho u v \\ \rho v^2 + p \\ v(E+p) \end{pmatrix} \qquad (3)$$

and $\vec{R}$ and $\vec{S}$ are the viscous flux vectors:

* Hypersonics Research Engineer, Member AIAA

N88-26336#

$$\vec{R} = \begin{pmatrix} 0 \\ \tau_{xx} \\ \tau_{xy} \\ u\tau_{xx} + v\tau_{xy} - \frac{K}{\beta_r Pr}\frac{\partial T}{\partial x} \end{pmatrix} \quad (4)$$

$$\vec{S} = \begin{pmatrix} 0 \\ \tau_{xy} \\ \tau_{yy} \\ u\tau_{xy} + v\tau_{yy} - \frac{K}{\beta_r Pr}\frac{\partial T}{\partial y} \end{pmatrix} \quad (5)$$

where $\tau_{xx} = (\lambda + 2\mu)u_x + \lambda v_y$, $\tau_{xy} = \mu(u_y + v_x)$, and $\tau_{yy} = (\lambda + 2\mu)v_y + \lambda u_x$.

The original formulation assumed the gas to be calorically perfect and thermally perfect[2]. This assumption results in a simple algebraic relationship between the pressure, temperature and flux variables, namely

$$P = (\gamma - 1)\Big(q_4 - \frac{\frac{1}{2}(q_2^2 + q_3^2)}{q_1}\Big) \quad (6)$$

$$T = \gamma(\gamma - 1)\Big(\frac{q_4}{q_1} - \frac{\frac{1}{2}(q_2^2 + q_3^2)}{q_1^2}\Big) \quad (7)$$

where γ is constant. For a gas where the specific heats are variable and the gas follows the ideal equation of state, the pressure and temperature are interrelated through the definition of the enthalpy,

$$\begin{aligned} h(T) &= \Sigma\, y_i\, h_i(T) \\ &= \int_{Tr}^{T} C_p\, dT + \Delta h_f^0 \\ &= e + \frac{P}{\rho} \end{aligned} \quad (8)$$

where y_i is the mass fraction of the i-th constituent of the gas. By assuming the ideal gas equation of state, eqn. (8) is manipulated and written in terms of the flux variables as

$$h(T) - RT = \frac{q_4}{q_1} - \frac{1}{2}\Big[\Big(\frac{q_2}{q_1}\Big)^2 + \Big(\frac{q_3}{q_1}\Big)^2\Big] \quad (9)$$

For this analysis, the thermodynamic data for C_p and h are in the form of polynomials in temperature for each species of the ideal gas mixture. These data have been calculated by statistical mechanics for the temperature range of 200 to 15000 Kelvin for the species N, NO, N2, O, N, O2, e-, N+, NO+, O+, N2+ and O2+[6,7,8,9,10]. The functional form for the specific heat and enthalpy of each species is

$$\Big(\frac{C_p}{R}\Big)_i = a_1 + a_2 T + a_3 T^2 + a_4 T^3 + a_5 T^4 \quad (10)$$

$$\Big(\frac{h}{RT}\Big)_i = a_1 + \frac{a_2}{2}T + \frac{a_3}{3}T^2 + \frac{a_4}{4}T^3 + \frac{a_5}{5}T^4 + a_6 \quad (11)$$

The polynomials use two sets of coefficients valid on the ranges of 200>T>5000 and 5000>T>15000 Kelvin and are constrained to match at the midpoint temperature of 5000 Kelvin. Once the chemical composition is known, eqn. (9) is solved iteratively for the temperature using a Newton-Raphson iteration, which then yields the pressure through the ideal gas equation of state. To calculate the derivatives of pressure needed in the flux jacobians an effective gamma approach is used similar to the methods presented in references 11 and 12. The boundary condtion routines for slip, no-slip adiabatic and specified temperature walls were modified to be consistent with the thermodynamics and resulting equation of state. For frozen flows, the chemical composition is held constant throughout the flowfield at the standard air composition, while for the equilibrium air calculations the species solutions are obtained separately using an equilibrium solver.

CHEMICAL EQUILIBRIUM SOLVER

The species and thermodynamic solutions needed for the equilibrium air calculations are obtained in a "black box" fashion using the newly developed equilibrium air package developed at NASA Lewis by McBride et. al.[6]. This package is based on a Helmholtz free energy minimization procedure fully described by Gordon and McBride in reference 13. This package requires only the local density and internal energy (which are simply related to the flux variables) as input, and returns as output the resultant pressure, temperature, equilibrium speed of sound γ_e and chemical composition. The chemical composition is then used in a consistent manner to compute the needed thermodynamic properties. A special procedure is used to initialize the chemical equilibrium calculations as well as a procedure to determine freezing conditions. The development of this unique equilibrium solver is still underway. A more complete description of the package, procedures and governing relations is available in reference 6.

RESULTS

To demonstrate the new capability of this solver, calculations of a variety of geometries and flight conditions are presented. Comparisons are made between the calorically perfect, thermally perfect and chemical equilibrium air calculations for these hypersonic flows.

(1) $M_\infty = 7$ Hypersonic Ramp Case

Mach 7 flow over a 15° ramp is calculated at a freestream pressure of 1 atmosphere and temperature of 350 Kelvin. To highlight the real gas upgrades an adiabiatic wall boundary condition was chosen for this laminar calculation. A simple sheared grid was used with clustering along the lower wall for this 100 (axially) by 50 (normally) grid. The upper boundary was treated as a symmetry plane. Figure 1 shows the computed pressure contours for the calorically perfect calculation while Figures 2 and 3 compare the wall pressures and temperatures (respectively) for the three different thermo-chemistry modes. Figure 4 indicates the amount of dissociation calculated in the equilibrium calculation by showing the amount of NO along the wall. The L2 norm of the residuals was driven down by over 4 orders of magnitude in approximately 2000 iterations for the three different calculations.

The pressure contours in Figure 1 show the leading edge shock merging with the ramp shocks, and the shock/shock interraction of the upper and lower ramp shocks. Examination of Figures 2 and 3 shows marked differences in both wall pressure and temperature between the non-real gas and the real gas calculations. The calorically perfect calculation (C_p=constant) indicates a small separation/interraction region extending approximately 0.2 meters ahead of the ramp turn (the ramp turn is located at X=0.3 meters). This separation/interraction region is shortened considerably in the frozen air (variable C_p) and equilibrium air calculations. It appears that by accounting for more thermodynamic degrees of freedom a larger turning angle could be accepted by the flow before separating. After the initial temperature and pressure rise caused by the ramp, it is interesting to notice that the frozen air and equilibrium air wall temperatures are fairly close, while the calorically perfect wall temperature is much higher for this lower Mach number case.

(2) $M_\infty = 10$ Hypersonic Ramp Case

A Mach 10, 10° ramp case was calculated with freestream conditions of 1 atmosphere pressure and 300 Kelvin temperature. This case was also run laminar and with an adiabatic wall to highlight the real gas effects. The same grid dimensions and near wall stretching used in the Mach 7 case were used for this calculation. The L2 norm of the residuals was driven down by over 4 orders of magnitude in approximately 4000 iterations for all three different thermo-chemistry modes.

Figure 5 illustrates the computed pressure contours for the calorically perfect calculation, while Figures 6 and 7 show the wall pressure and temperature comparison between the three thermo-chemistry modes. The extent of air dissociation is indicated in Figure 8 which shows the computed mass fractions of NO along the wall. Examination of the pressure and temperature plots indicates a fairly large separation region ahead of the ramp for the calorically perfect calculation with a milder pressure rise profile. The frozen and equilibrium calculations show a progressively smaller interraction region with a sharper pressure rise. In this case, the final wall temperatures indicate a much larger difference between the calorically perfect, frozen air and equilibrium air calculations. The amount of dissociation is nearly twice that of the Mach 7 case which is indicated by the fairly high amount of NO present at the wall.

(3) P2 Hypersonic Inlet at $M_\infty = 10$, H=100 Kft.

The P2 inlet geometry, taken from reference 14, was used to represent a large scale inlet at a flight Mach number of 10 at an altitude of 100,000 feet. For this Mach number and altitude the Reynolds number is low enough to assume that the flow is initially laminar, and to remove any issues about transition to turbulence and the correct modelling of the turbulence, the flow is considered to remain laminar along the length of the inlet. It is also assumed that the wall temperature remains constant at 1000 Kelvin. A 100 by 80 grid was used with near wall clustering on both the ramp and cowl walls. Figure 9 shows the pressure contours calculated in the calorically perfect gas mode. The comparisons between the different thermochemistry calcultions for the ramp and cowl pressures and temperatures are shown in Figures 10 and 11, respectively. Figure 12 compares the computed exit plane temperature profiles between the three different calculations. For the calorically perfect and frozen air calculations the L2 norm of the residuals was driven down by over 4 orders of magnitude in approximately 5000 iterations while the equilibrium calculation residual was driven down only 3 orders.

Examination of the ramp and cowl pressure comparisons (Figures 10 and 11) shows little difference between the different thermo-chemistry modes. The exit plane temperature profiles show minor differences in the temperature peaks and in the core flow regions. These results show that for this relatively low hypersonic Mach number and for the "cooled" wall conditions that the real gas effects for this case are negligible.

SUMMARY AND CONCLUSIONS

A two dimensional steady state Navier)Stokes flow solver has been modified to account for real gas effects and has been demonstrated on various geometries at hypersonic Mach numbers. The chemically frozen air modifications account for the variation of the air thermodynamics using polynomials in temperature for the specific heats and enthalpies that are valid over the temperature range of 200 to 15,000 Kelvin. A specialized version of the NASA Lewis Chemical Equilibrium Code, CEC, was used to compute the chemical composition and resulting thermodynamic properties given a thermodynamic state specified by the flow code flux variables.

Three separate geometries and free stream Mach numbers and conditions were calculated and comparisons were made between the calorically perfect (C_p=constant), frozen air (variable C_p) and equilibrium air thermo-chemistry modes. Considerable differences were shown in wall pressures and temperatures for the two adiabatic wall hypersonic ramp cases. For these two cases, the adiabatic wall boundary conditions enabled the flow near the wall to reach near stagnation conditions, resulting in signifigant differences in the computed wall temperatures due to dissociation in the equilibrium calculations and to the variation of C_p in the frozen air calculations. The large scale inlet simulation showed negligible difference between the different thermo-chemistry modes. This is believed to be due to the specification of wall temperatures at levels low enough not to cause sufficient dissociation of the air. Although it cannot be extrapolated to higher Mach numbers or lower altitudes (resulting in higher stagnation conditions), it appears that for the large scale inlet case computed in this study little difference can be noted between the calorically perfect, frozen air and equilibrium air results.

ACKNOWLEDGEMENTS

This work was supported by NASA Lewis Research Center through contract NAS 3-24105, project monitor B. Anderson. The author is indebted to B. McBride and S.T. Yu for their permission to use the equilibrium air package, and to Dr. J. S. Shuen for his helpful comments and suggestions.

REFERENCES

[1.] Pulliam, T. H., and Steger, J. L. "Implicit Finite - Difference Simulations of Three Dimensional Compressible Flow." *AIAA Journal*, Vol. 18, No. 2, Feb. 1980, pp. 159- 167.

[2.] Cooper, G. K. "The PARC Code: Theory and Usage." AEDC-TR-87-24, October, 1987.

[3.] Beam, R. and Warming, R. F. "An Implicit Finite - Difference Algorithm for Hyperbolic Systems in Conservation - Law Form." *Journal of Computational Physics*, Vol. 22, No. 1, Sept. 1976, pp. 87-110.

[4.] Pulliam, T. H. "Euler and Thin Layer Navier-Stokes Codes: ARC2D, ARC3D." *Notes for Computational Fluid Dynamics User's Workshop*, The University of Tennessee Space Institute, Tullahoma, Tennessee, (UTSI Publication E02-4005-023-84), March 12-16, 1984, pp. 15.1-15.85.

[5.] Jameson, A., Schmidt, W., and Turkel, E. "Numerical Solutions of the Euler Equations by Finite Volume Methods Using Runge-Kutta Time-Stepping Schemes." AIAA Paper No. 81-1259, AIAA 14th Fluid and Plasma Dynamics Conference, Palo Alto, California, 1981.

[6.] Yu, S. T., McBride, B. J., Hsieh, K-C, and Shuen, J-S "Numerical Simulation of Hypersonic Inlet Flows with Equilibrium or Finite Rate Chemistry." AIAA-88-0273, January, 1988.

[7.] McBride, B. J., and Gordon, S. "FORTRAN IV Program for Calculations of Thermodynamic Data," NASA TN D-4097, 1967.

[8.] Moore, C., "Selected Tables of Atomic Spectra." NSRDS-NBS 3, 1975.

[9.] Moore, C., "Atomic Energy Levels." Vol 1, NSRDS-NBS 35, 1971.

[10.] Glushko, V. P., Gurvich, L. V., Bergman, G. A., Veyts, I. V., Medvedev, V. A., Khachkuruzov, G. A., and Yungman, V. S. "Thermodynamic Properties of Individual Substances." Academy of Sciences, Moscow, USSR, Vol 1, Parts 1 and 2, 1978.

[11.] Balakrishnan, A., Davy, W. C. and Lombard, C. K. "Real-Gas Flows about Three-Dimensional Configurations.", AIAA 83-0581, Jan, 1983.

[12] Shuen, J. S., and Yoon, S. "Numerical Study of Chemically Reacting Flows Using an LU Scheme." AIAA-88-0436, Jan, 1988.

[13.] Gordon, S., and McBride, B. J. "Computer Program for the Calculation of Complex Equilibrium Compositions, Rocket Performance, Incident and Reflected Shocks, and Chapman-Jouguet Detonations." NASA SP-273 Interim Revision, 1976.

[14.] Gnos, A.V., Watson, E. C., Seebaugh, W. R., Sanator, R. J. and DeCarlo, J. P. "Investigation of Flow Fields Within Large-Scale Hypersonic Inlet Models." NASA Tn D-7150, April, 1973.

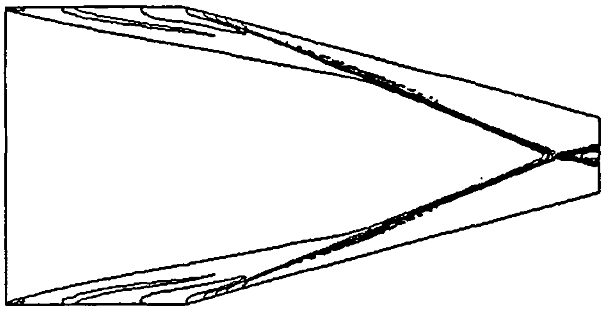

Figure 1. Pressure Contours, $M_\infty = 7$ Ramp Case

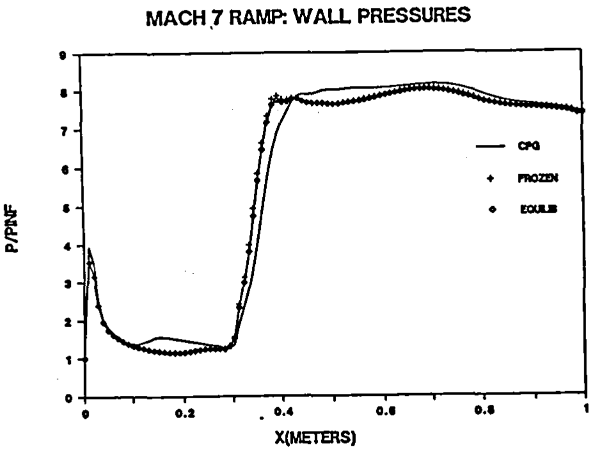

Figure 2. Wall Pressure Comparisons, $M_\infty = 7$ Ramp Case

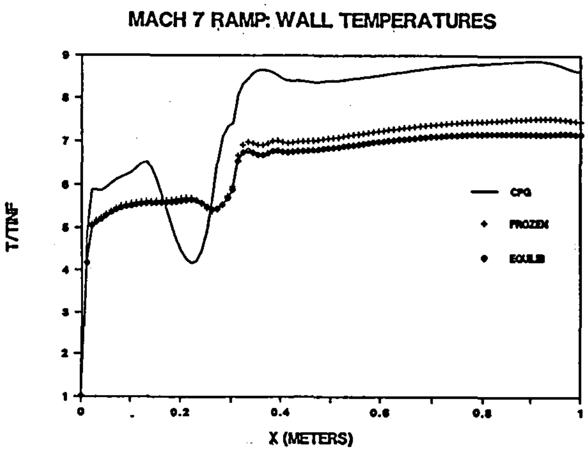

Figure 3. Wall Temperature Comparisons, $M_\infty = 7$ Ramp Case

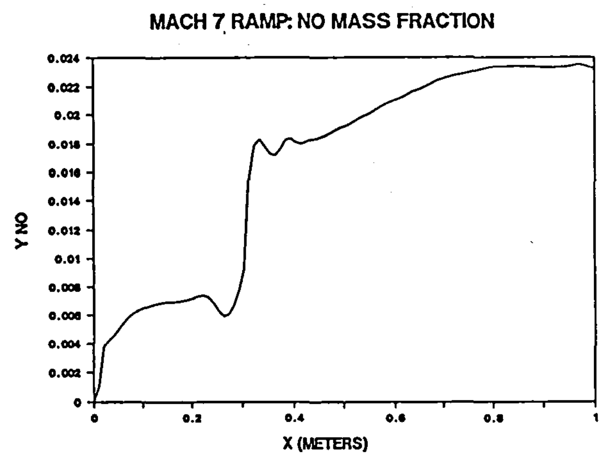

Figure 4. Wall NO Mass Faction, $M_\infty = 7$ Ramp Case

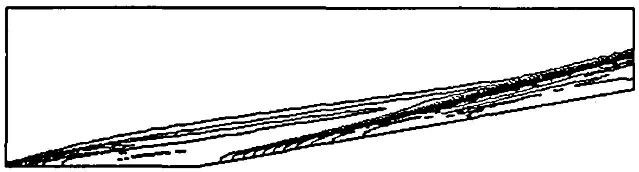

Figure 5. Pressure Contours, $M_\infty = 10$ Ramp Case

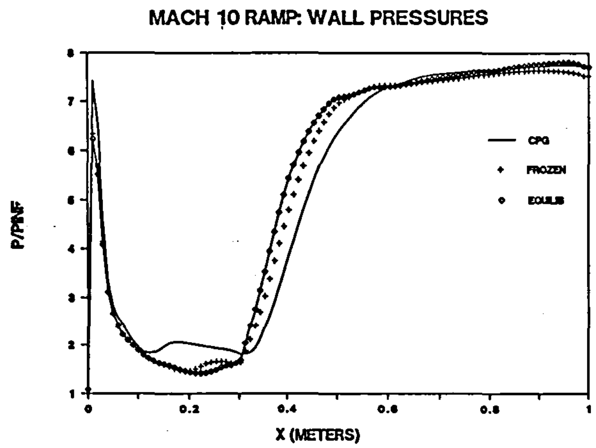

Figure 6. Wall Pressure Comparisons, $M_\infty = 10$ Ramp Case

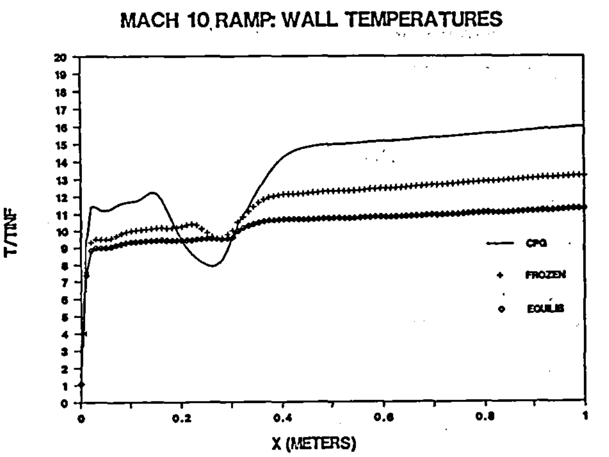

Figure 7. Wall Temperature Comparisons, $M_\infty = 10$ Ramp Case

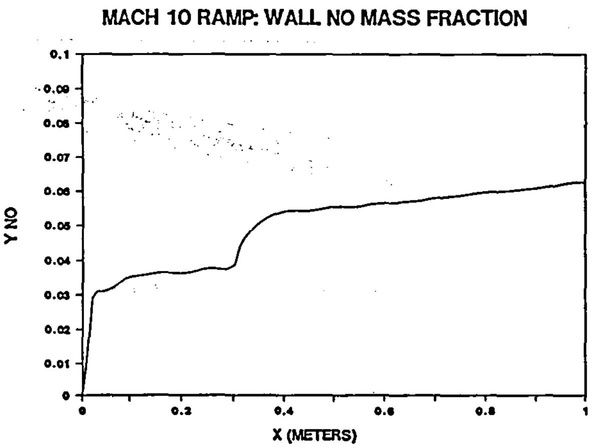

Figure 8. Wall NO Mass Fractions, $M_\infty = 10$ Ramp Case

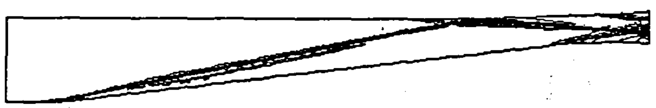

Figure 9. Pressure Contours, P2 Inlet Geometry, $M_\infty = 10$, H = 100 Kft

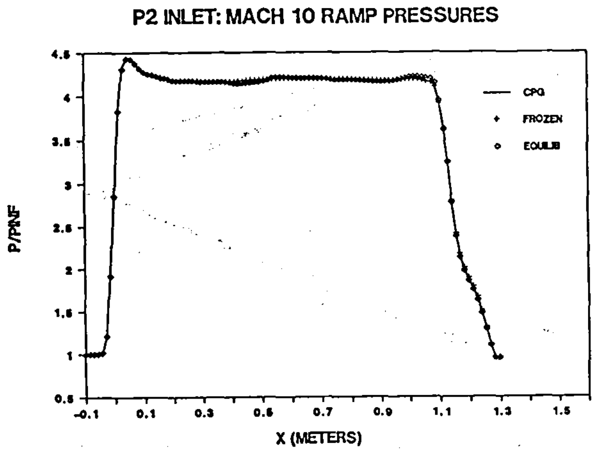

Figure 10. Ramp Pressures Comparisons, P2 Inlet Geometry, $M_\infty = 10$, H = 100 Kft

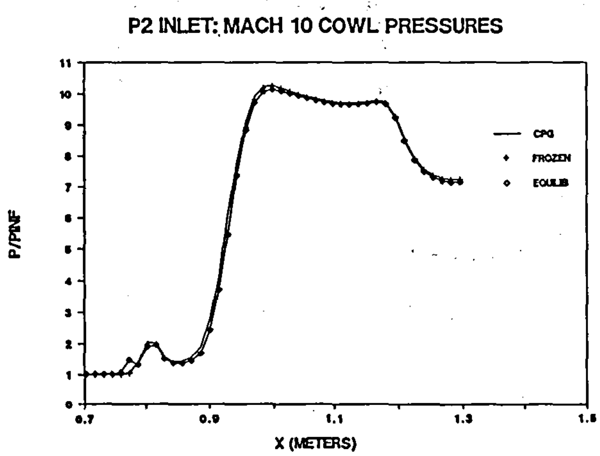

Figure 11. Cowl Pressurs Comparisons, P2 Inlet Geometry, $M_\infty = 10$, H = 100 Kft

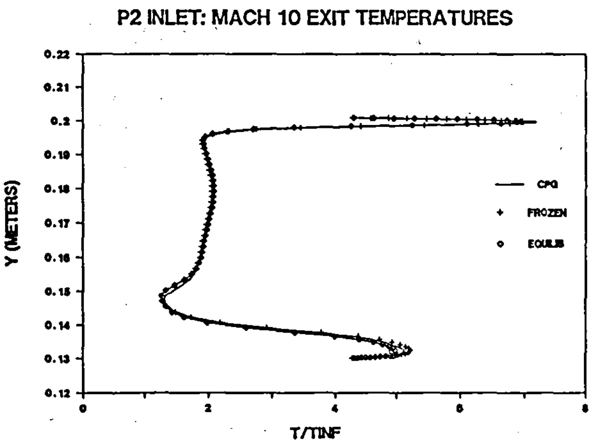

Figure 12. Exit Plane Temperature Profiles, P2 Inlet Geometry, $M_\infty = 10$, H = 100 Kft

Report Documentation Page

National Aeronautics and Space Administration

1. Report No. NASA CR-182167 AIAA-88-3076	2. Government Accession No.	3. Recipient's Catalog No.
4. Title and Subtitle: High Speed Inlet Calculations With Real Gas Effects		5. Report Date: July 1988
		6. Performing Organization Code
7. Author(s): William J. Coirier		8. Performing Organization Report No.: None (E-4287)
		10. Work Unit No.: 505-62-21
9. Performing Organization Name and Address: Sverdrup Technology, Inc. NASA Lewis Research Center Group Cleveland, Ohio 44135		11. Contract or Grant No.: NAS3-24105
12. Sponsoring Agency Name and Address: National Aeronautics and Space Administration Lewis Research Center Cleveland, Ohio 44135-3191		13. Type of Report and Period Covered: Contractor Report Final
		14. Sponsoring Agency Code

15. Supplementary Notes

Project Manager, Bernard H. Anderson, Internal Fluid Mechanics Division, NASA Lewis Research Center. Prepared for the 24th Joint Propulsion Conference cosponsored by the AIAA, ASME, SAE, and ASEE, Boston, Massachusetts, July 11-13, 1988.

16. Abstract

A two-dimensional steady-state Navier-Stokes solver has been upgraded to include the effects of frozen and equilibrium air chemistry for applications to high speed flight vehicles. To provide a computationally economical first order approximation to the high temperature physics, variable thermodynamic data is used for the chemically frozen mode to allow for a variation with temperature of the air specific heats and enthalpy. For calculations involving air in chemical equilibrium, a specially modified version of the NASA Lewis Chemical Equilibrium Code, CEC, is used to compute the chemical composition and resultant thermochemical properties. The upgraded solver is demonstrated by comparing results from calorically perfect (C_p = constant), thermally perfect (frozen) and equilibrium air calculations for a variety of geometries, and flight Mach numbers.

17. Key Words (Suggested by Author(s)): High speed inlet calculations; Chemically frozen air; Chemical equilibrium air	18. Distribution Statement: Unclassified – Unlimited; Subject Category 02

19. Security Classif. (of this report)	20. Security Classif. (of this page)	21. No of pages	22. Price*
Unclassified	Unclassified	7	A02

NASA FORM 1626 OCT 86

*For sale by the National Technical Information Service, Springfield, Virginia 22161

End of Document